EUSIPCO 2013 1569741431

COMPUTATIONALLY EFFICIENT DAMPED CAPON AND APES SPECTRAL ESTIMATION

George-Othon Glentis[*] *and Andreas Jakobsson*[†]

[*]University of Peloponnese, Dept. Telecommunications, Greece
[†]Mathematical Statistics, Lund University, Sweden

ABSTRACT

In this paper, we introduce computationally efficient implementations of the data-dependent non-parametric damped Capon (dCapon) and APES (dAPES) spectral estimators. These estimators form two-dimensional frequency representations over both frequency and damping, and have been shown to enable an efficient separation of closely spaced spectral lines with different line widths. The proposed implementations are formed using an FFT-based fast polynomial reformulation exploiting the displacement structure of the matrices associated with the trigonometric polynomials that appear in the nominator and the denominator of the spectral estimators. The resulting implementations are exact and notably reduces the required computational complexity of the estimators. Numerical simulations illustrates the performance and the achieved complexity gain of the proposed implementations.

Index Terms— Spectral estimation, damped sinusoidals, Capon, APES, computationally efficient implementations

1. INTRODUCTION

In a wide variety applications, the signal of interest may be well modeled as consisting of a sum of decaying sinusoidal signals, wherein one has an interest of estimating both the frequencies and the decays of the signal components (see, e.g., [1–6] and the references therein). Consider a signal, $x(n)$, consisting of d decaying sinusoidal signals corrupted by an additive noise, $w(n)$, typically representing both the measurement noise and the inherent modeling error, such that

$$x(n) = \sum_{k=1}^{d} \alpha_k e^{-\beta_k n + \jmath\omega_k n} + w(n) \qquad (1)$$

where $n = 1, \ldots, N$, and $\alpha_k \in \mathcal{C}$, $\beta_k > 0$, and $\omega_k \in (0, 2\pi]$ denote the amplitudes, damping factors, and the (angular) frequencies of the kth component, respectively. In some cases, the number of decaying modes, d, is known, whereas in other cases it is unknown and must therefore be estimated from the available measurements; herein, we are concerned with this latter, more general, problem, treating d as unknown, as well as posing no strong *a priori* assumption on the color of the additive noise. It often happens in, e.g., spectroscopic applications, that the decaying modes are closely spaced in frequency, but exhibit notably different damping factors, implying that the spectral lines will have different line width. The resulting spectral peaks are thus often overlapping, making it difficult both to distinguish the weaker modes, as well as corrupting the estimates of the component's damping constants, which are often formed as the peak width at half the peak height. To address this problem, the non-parametric damped Capon (dCapon) and APES (dAPES) spectral estimation techniques were introduced in [1] to form two-dimensional (2-D) representations of the spectral distribution over frequency and damping, thereby effectively allowing for a separation of modes being closely spaced in frequency, but having notable different line widths. This concept was there found to well separate the modes, and the concept has since been both applied and generalized to other forms of 2-D representations [6–8]. Although both the Capon and APES spectral estimators may be efficiently implemented for a given damping constant using methods reminiscent to the ones developed in [9–12], the damped estimators as such are computationally cumbersome as no similar speed-up has been developed for the evaluation of the estimators over also the damping dimension. Such an efficient implementation is the topic of this work, wherein we introduce fast polynomial implementations of both the dCapon and dAPES estimators, exploiting efficient Gohberg-Semencul (GS) style formulations for the required matrix products and inverses, thereby reducing the required computational complexity dramatically.

The work of A. Jakobsson was supported in part by the Swedish Research Council and Carl Trygger's foundation.

2. THE DAMPED CAPON AND APES ESTIMATORS

In this section, we briefly review the dCapon and dAPES spectral estimators, as well as introduce polynomial formulations of the estimators reminiscent to the ones introduced in [13, 14]. Following the matched filter bank framework, dividing the observation into L sub-vectors,

$$\mathbf{x}_M(n) = \left[\begin{array}{cccc} x(n) & x(n+1) & \ldots & x(n+M-1) \end{array} \right]^T \qquad (2)$$

for $n = 1, \ldots, L$, where $L = N - M + 1$, these are filtered through a set of data-adaptive filters formed such that each is passing a given frequency and damping, say (ω, β), undistorted, whereas the power from all other frequencies and dampings are suppressed as much as possible by the filter. Thus, the filter output may be written as

$$\mathbf{h}_{\omega,\beta}^{*}\mathbf{x}_M(n) = \alpha e^{-\beta n + \jmath\omega n} + \bar{w}(n) \tag{3}$$

where $(\cdot)^*$ denotes the conjugate transpose, and $\bar{w}(n)$ the filtered noise process, containing both the contributions from the additive (potentially colored) noise and the filtered modes from all other frequencies and dampings than (ω, β), implying that the 2-D least-squares *energy* spectral estimate at (ω, β) may be formed as [1](see also [4])

$$\hat{\phi}_{\omega,\beta} = \gamma_{N,\beta} \left|\hat{\alpha}_{\omega,\beta}\right|^2 \tag{4}$$

where

$$\begin{aligned}
\hat{\alpha}_{\omega,\beta} &= \mathbf{h}_{\omega,\beta}^{*}\mathbf{g}_{\omega,\beta} && (5)\\
\mathbf{g}_{\omega,\beta} &= \frac{1}{\gamma_{L,\beta}} \sum_{n=1}^{L} \Big\{ \mathbf{x}_M(n) e^{-\beta n} \Big\} e^{-\jmath\omega n} && (6)\\
\gamma_{\ell,\beta} &= \sum_{n=1}^{\ell} e^{-2\beta n} = e^{-2\beta} \frac{e^{-2\beta\ell} - 1}{e^{-2\beta} - 1} && (7)
\end{aligned}$$

with the data-adaptive filters, $\mathbf{h}_{\omega,\beta}$, being formed as either the Capon- or APES-based filters

$$\begin{aligned}
\mathbf{h}_{\omega,\beta}^{C} &= \frac{\hat{\mathbf{R}}_x^{-1}\mathbf{s}_M(\omega,\beta)}{\mathbf{s}_M^{*}(\omega,\beta)\hat{\mathbf{R}}_x^{-1}\mathbf{s}_M(\omega,\beta)} && (8)\\
\mathbf{h}_{\omega,\beta}^{A} &= \frac{\hat{\mathbf{Q}}_{\omega,\beta}^{-1}\mathbf{s}_M(\omega,\beta)}{\mathbf{s}_M^{*}(\omega,\beta)\hat{\mathbf{Q}}_{\omega,\beta}^{-1}\mathbf{s}_M(\omega,\beta)} && (9)
\end{aligned}$$

where $\mathbf{s}_\ell(\omega, \beta)$ denotes the $\ell \times 1$ (damped) Fourier vector

$$\mathbf{s}_\ell(\omega,\beta) = \left[\begin{array}{cccc} 1 & z_{\omega,\beta} & \ldots & z_{\omega,\beta}^{\ell-1} \end{array}\right]^T \tag{10}$$

with $z_{\omega,\beta} = e^{-\beta+\jmath\omega}$, and where $\hat{\mathbf{R}}_x$ denotes an estimate of the sample covariance matrix of $\mathbf{x}_M(t)$, typically formed as

$$\hat{\mathbf{R}}_x = \sum_{\ell=1}^{L} \mathbf{x}_M(\ell)\mathbf{x}_M^{*}(\ell) \tag{11}$$

and $\hat{\mathbf{Q}}_{\omega,\beta}$ is an estimate of the (frequency and damping dependent) noise covariance matrix formed as

$$\hat{\mathbf{Q}}_{\omega,\beta} = \hat{\mathbf{R}}_x - \gamma_{L,\beta}\mathbf{g}_{\omega,\beta}\mathbf{g}_{\omega,\beta}^{*} \tag{12}$$

which, by exploiting the matrix inversion lemma, implies that

$$\hat{\mathbf{Q}}_{\omega,\beta}^{-1} = \hat{\mathbf{R}}_x^{-1} + \frac{\gamma_{L,\beta}\hat{\mathbf{R}}_x^{-1}\mathbf{g}_{\omega,\beta}\mathbf{g}_{\omega,\beta}^{*}\hat{\mathbf{R}}_x^{-1}}{1 - \gamma_{L,\beta}\mathbf{g}_{\omega,\beta}^{*}\hat{\mathbf{R}}_x^{-1}\mathbf{g}_{\omega,\beta}} \tag{13}$$

In order form an estimate of the energy spectrum, one thus computes (4), in combination of either (8) or (9), over the range of frequencies and dampings of interest. Reminiscent to the Capon and APES formulation derived in [13, 14] (see also [12]), this then allows the dCapon and dAPES estimates to be formed as

$$\begin{aligned}
\hat{\phi}_{\omega,\beta}^{C} &= \gamma_{N,\beta} \left| \frac{\varphi_{\omega,\beta}^{G}}{\varphi_{\omega,\beta}^{R}} \right|^2 && (14)\\
\hat{\phi}_{\omega,\beta}^{A} &= \frac{\gamma_{N,\beta} \left|\varphi_{\omega,\beta}^{G}\right|^2}{\left| \left(1 - \gamma_{L,\beta}\varphi_{\omega,\beta}^{H}\right) \varphi_{\omega,\beta}^{R} + \gamma_{L,\beta} \left|\varphi_{\omega,\beta}^{G}\right|^2 \right|^2} && (15)
\end{aligned}$$

where

$$\begin{aligned}
\varphi_{\omega,\beta}^{R} &\triangleq \mathbf{s}_M^{*}(\omega,\beta)\hat{\mathbf{R}}_x^{-1}\mathbf{s}_M(\omega,\beta) && (16)\\
\varphi_{\omega,\beta}^{G} &\triangleq \frac{z_{-\omega,\beta}}{\gamma_{L,\beta}} \mathbf{s}_M^{*}(\omega,\beta)\hat{\mathbf{G}}_x\mathbf{s}_L(-\omega,\beta) && (17)\\
\varphi_{\omega,\beta}^{H} &\triangleq \frac{e^{-2\beta}}{\gamma_{L,\beta}^2} \mathbf{s}_L^{*}(\omega,\beta)\hat{\mathbf{H}}_x\mathbf{s}_L(\omega,\beta) && (18)
\end{aligned}$$

with

$$\begin{aligned}
\hat{\mathbf{G}}_x &\triangleq \hat{\mathbf{R}}_x^{-1}\hat{\mathbf{X}} && (19)\\
\hat{\mathbf{H}}_x &\triangleq \hat{\mathbf{X}}^{*}\hat{\mathbf{G}}_x && (20)
\end{aligned}$$

and where $\hat{\mathbf{X}}$ denotes the Hankel-structured data matrix

$$\hat{\mathbf{X}} = \left[\begin{array}{ccc} \mathbf{x}_M(1) & \ldots & \mathbf{x}_M(L) \end{array}\right] \tag{21}$$

Clearly, should one instead wish to form an estimate of the amplitude spectrum, $|\hat{\alpha}_{\omega,\beta}|$, this can be formed similarly. Comparing the resulting expressions with the Capon and APES estimators, formed only over frequencies, one may note that the addition of the damping component prevents an efficient implementation along the lines of [9–12], although similar formulations may be used for each given damping component. In the following, we proceed to examine how these expressions may reformulated to also allow for an efficient implementation over the damping dimension.

3. FAST POLYNOMIAL IMPLEMENTATION

In order to form fast implementations of (16)-(18), we reformulate these expressions so that they have a close-to-Toeplitz structure rather than their current close-to-Hankel structure, using the Hankel to Toeplitz mapping

$$\mathbf{X} \triangleq \mathbf{J}_M\hat{\mathbf{X}} \tag{22}$$

with $\mathbf{J}_M$ denoting the exchange matrix of appropriate dimensions, implying that

$$\begin{aligned}
\hat{\mathbf{R}}_x &= \mathbf{J}_M\mathbf{R}_x\mathbf{J}_M && (23)\\
\hat{\mathbf{G}}_x &= \mathbf{J}_M\,\mathbf{G}_x && (24)
\end{aligned}$$

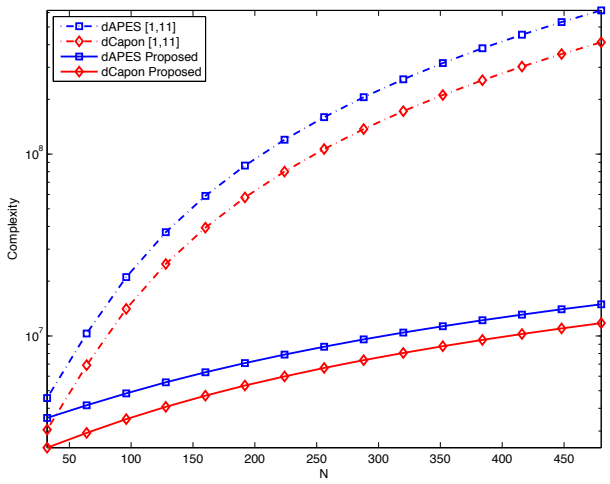

Fig. 1. Computational complexity of the proposed dCapon and dAPES implementations as compared to the implementations presented in [1, 11], for $M = N/2 - 1$, $K = 1024$, and $D = 200$.

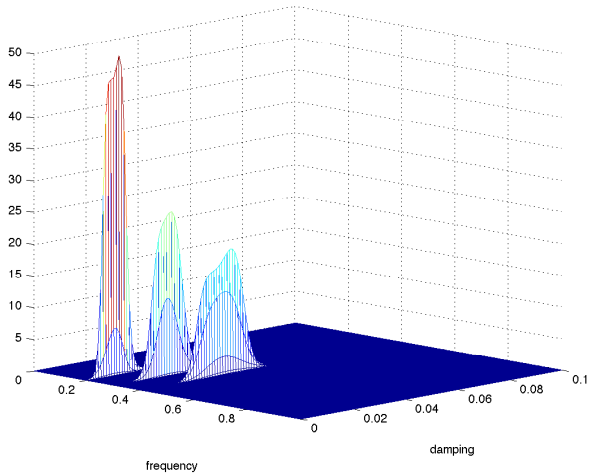

Fig. 2. An illustration of the dAPES estimate for three damped sinusoidal signals.

as well as $\hat{\mathbf{H}}_x = \mathbf{H}_x$, where

$$\mathbf{R}_x = \mathbf{X}\mathbf{X}^* \quad (25)$$
$$\mathbf{G}_x = \mathbf{R}_x^{-1}\mathbf{X} \quad (26)$$
$$\mathbf{H}_x = \mathbf{X}^*\mathbf{G}_x \quad (27)$$

which allows us to express (16)-(18) as

$$\varphi^R_{\omega,\beta} = \mathbf{s}^*_M(-\omega,-\beta)\mathbf{R}_x^{-1}\mathbf{s}_M(-\omega,-\beta)e^{-2\beta(M-1)}$$
$$\varphi^G_{\omega,\beta} = \frac{z_{-\omega,\beta}}{\gamma_{L,\beta}}\,\mathbf{s}^*_M(-\omega,-\beta)\mathbf{G}_x\mathbf{s}_L(-\omega,\beta)e^{(-\beta+\jmath\omega)(M-1)}$$
$$\varphi^H_{\omega,\beta} = \frac{e^{-2\beta}}{\gamma^2_{L,\beta}}\,\mathbf{s}^*_L(\omega,\beta)\mathbf{H}_x\mathbf{s}_L(\omega,\beta)$$

Clearly, $\mathbf{R}_x$ is now a close-to-Toeplitz matrix, implying that its inverse, $\mathbf{R}_x^{-1}$, as well as the associated matrices $\mathbf{G}_x$ and $\mathbf{H}_x$ are also close-to-Toeplitz matrices, thereby enjoying GS representations of the form [12]

$$\mathbf{R}_x^{-1} = \sum_{i=1}^{4}\sigma_i\mathcal{L}_M\left(\mathbf{t}^i_M\right)\mathcal{L}^*_M\left(\mathbf{t}^i_M\right) \quad (28)$$
$$\mathbf{G}_x = \sum_{i=1}^{4}\sigma_i\mathcal{L}_M\left(\mathbf{t}^i_M\right)\mathcal{L}^*_{L,M}\left(\mathbf{v}^i_L\right) \quad (29)$$
$$\mathbf{H}_x = \sum_{i=1}^{4}\sigma_i\mathcal{L}_L\left(\mathbf{v}^i_L\right)\mathcal{L}^*_L\left(\mathbf{v}^i_L\right) \quad (30)$$

for a set of properly chosen vectors $\mathbf{t}^i_M$ and $\mathbf{v}^i_L$, and integers $\sigma_i \in \{-1, 1\}$, for $i = 1, 2, 3, 4$, with $\mathcal{L}_M(\mathbf{y})$ denoting an $M \times M$ lower triangular Toeplitz matrix whose first column equals to $\mathbf{y}$, such that

$$\mathcal{L}_M(\mathbf{y}) = \begin{bmatrix} \mathbf{y}_0 & 0 & \dots & 0 \\ \mathbf{y}_1 & \mathbf{y}_0 & \ddots & \vdots \\ \vdots & \ddots & \ddots & \vdots \\ \mathbf{y}_{M-1} & \dots & \mathbf{y}_1 & \mathbf{y}_0 \end{bmatrix} \quad (31)$$

where $\mathbf{y}_k$ indicates the kth index in the (generic) $M\times 1$ vector $\mathbf{y}$, and with $\mathcal{L}_{L,M}(\mathbf{y})$ denoting an $L \times M$ truncated version of $\mathcal{L}_L(\mathbf{y})$. Consider a trigonometric polynomial of the form

$$\psi_{\omega,\lambda}(\mathbf{y}_M) \triangleq \mathbf{f}^*_M(\omega,\lambda)\mathcal{L}_M\left(\mathbf{y}_M\right)\mathcal{L}^*_M\left(\mathbf{y}_M\right)\mathbf{f}_M(\omega,\lambda) \quad (32)$$

where

$$\mathbf{f}_M(\omega,\lambda) \triangleq \begin{bmatrix} 1 & \lambda e^{\jmath\omega} & \dots & \lambda^{M-1}e^{\jmath\omega(M-1)} \end{bmatrix}^T \quad (33)$$

This implies (34), given at the top of the following page, with $\mathbf{Z}_M$ denoting the $M \times M$ down-shifting matrix, and where

$$\mathbf{y}_M(\lambda) \triangleq \mathbf{y}_M \odot \mathbf{f}_M(0,\lambda) \quad (35)$$

allowing $\psi_{\omega,\lambda}$ to be efficiently computed using the FFT as

$$\psi_{\omega,\lambda}(\mathbf{y}_M) = \sum_{\ell=-M+1}^{M-1} c_\ell(\lambda)e^{\jmath\omega\ell} \quad (36)$$

where

$$[c_{M-1}(\lambda)\; c_{M-2}(\lambda)\; \dots c_0(\lambda)]^T = \mathcal{L}_M\left(\mathbf{y}_M(\lambda)\right)\mathbf{u}_M(\lambda) \quad (37)$$

with $c_{-\ell}(\lambda) = c^*_\ell(\lambda)$, and

$$\mathbf{u}_M(\lambda) \triangleq \mathrm{conj}\Big[\mathbf{J}_M\mathbf{y}_M\Big] \odot \boldsymbol{\mu}_M(\lambda) \quad (38)$$

$$\psi_{\omega,\lambda}(\mathbf{x}_M) = \sum_{\kappa=0}^{M-1} \mathbf{f}_M^*(\omega,\lambda)\mathbf{Z}_M^\kappa \mathbf{y}_M \left(\mathbf{Z}_M^\kappa \mathbf{y}_M\right)^* \mathbf{f}_M(\omega,\lambda) = \sum_{\kappa=0}^{M-1} \lambda^{2\kappa} \mathbf{f}_M^*(\omega,0)\mathbf{Z}_M^\kappa \mathbf{y}_M(\lambda) \left(\mathbf{Z}_M^\kappa\ \mathbf{y}_M(\lambda)\right)^* \mathbf{f}_M(\omega,0) \quad (34)$$

where $\odot$ denotes the Schur-Hadamard (element wise) product, and with the kth element of $\boldsymbol{\mu}_M(\lambda)$ being computed as

$$[\boldsymbol{\mu}_M(\lambda)]_k = \sum_{\ell=0}^{\kappa} \lambda^{2\ell} \quad (39)$$

Furthermore, consider a trigonometric polynomial of the form

$$\xi_{\omega,\lambda}(\mathbf{y}_M, \mathbf{w}_L) \triangleq \mathbf{f}_M^*(\omega,\lambda)\mathcal{L}_M\left(\mathbf{y}_M\right)\mathcal{L}_{L,M}^*\left(\mathbf{w}_L\right)\mathbf{f}_L(\omega,\lambda^{-1}) \quad (40)$$

which, reminiscent to (34), may be expressed as (41), given at the top of the following page, which implies that the coefficients of the trigonometric polynomial $\xi_{\omega,\lambda}$ can be computed exactly as stated in Lemma 1 in [12], being applied on the modified vectors $\mathbf{y}_M(\lambda)$ and $\mathbf{w}_L(\lambda^{-1})$, defined by (35) and by

$$\mathbf{w}_L(\lambda^{-1}) \triangleq \mathbf{w}_L \odot \mathbf{f}_M(0,\lambda^{-1}) \quad (42)$$

respectively. Exploiting these expressions, one may efficiently compute (16)-(18) as

$$\varphi_{\omega,\beta}^R = e^{-2\beta(M-1)} \sum_{i=1}^{4} \sigma_i \psi_{-\omega,e^\beta}(\mathbf{t}_M^i) \quad (43)$$

$$\varphi_{\omega,\beta}^G = \frac{z_{-\omega,\beta}}{\gamma_{L,\beta}} \sum_{i=1}^{4} \sigma_i \xi_{-\omega,e^\beta}(\mathbf{t}_M^i, \mathbf{v}_L^i) \quad (44)$$

$$\varphi_{\omega,\beta}^H = \frac{e^{-2\beta}}{\gamma_{L,\beta}^2} \sum_{i=1}^{4} \sigma_i \psi_{\omega,e^{-\beta}}(\mathbf{v}_L^i) \quad (45)$$

where the vectors $\mathbf{t}_M^i$ and $\mathbf{v}_L^i$, as well as scalars σ_i, $i = 1,2,3,4$, are estimated from the measurement $x(n)$, for $n = 1,\ldots,N$, by means of the fast generalized Levinson algorithm, presented in [12], at a cost of $\mathcal{O}(M^2)+\mathcal{O}(N\log_2(N))$ operations. With these, the coefficients of the trigonometric polynomials $\psi_{\omega,\lambda}(\mathbf{y}_M)$ and $\xi_{\omega,\lambda}(\mathbf{y}_M,\mathbf{w}_L)$, as defined in (32) and (40), are estimated using the fast Toeplitz vector multiplication method, contributing to an overall cost of $D\cdot\mathcal{O}(N\log_2(N))$ operations, where D is the dimension of the damping grid. With these, the polynomials in (43)-(45) may then be evaluated on the unit circle at a cost of $D\cdot\mathcal{O}(K\log_2(K)$ operations, where K is the dimension of the (equally spaced) frequency grid. Summarizing the above computational complexity, the proposed fast implementations of the dCapon and the dAPES estimates requires, approximately,

$$C^{new} = \mathcal{O}(M^2) + D\Big[\mathcal{O}\left(N\log_2(N)\right) + \mathcal{O}\left(K\log_2(K)\right)\Big]$$

operations, which is considerably lower than the complexity of the scheme suggested in [1], which exploits the efficient scheme presented in [11] for the evaluation of the spectra for each separate damping constant, requiring, approximately,

$$C^{[12]} = \mathcal{O}(M^2) + D\Big[\mathcal{O}\left(MN\log_2(N)\right) + \mathcal{O}\left(K\log_2(K)\right)\Big]$$

operations.

4. NUMERICAL SIMULATIONS

The computational performance gain of the proposed (exact) implementations is illustrated in Figure 1, where we examine the (theoretical) complexity of the proposed implementations as a function of the number of samples, N, using a filter length of $M = N/2-1$ taps, and evaluating the performance over a frequency and damping grid having $K = 1024$ and $D = 200$ grid points, respectively, as compared with the (theoretical) complexity of the implementations proposed in [1], exploiting [11], clearly illustrating the dramatic complexity gain, even for cases of quite limited data dimensions. To make a simple illustration the performance of the estimators, Figure 2 illustrates the dAPES estimate for a signal consisting of three unit amplitude sinusoidal signals with (absolute) frequencies and dampings $(f_1,\beta_1) = (0.2,-0.01)$, $(f_2,\beta_2) = (0.3,-0.02)$, and $(f_3,\beta_3) = (0.4,-0.03)$, respectively. As seen in the figure, the 2-D spectrum clearly separates the peaks in both the frequency and damping dimensions, and, as expected, exhibits lower energy peaks for the more damped sinusoids. Should one be interested in the amplitudes of the decaying components, this can easily be found using the corresponding amplitude estimates, which will then have peaks close to unity. The reader is referred to [1] for a more detailed and thorough study of the performance of the estimators.

5. CONCLUSIONS

In this work, we have introduced computationally efficient exact implementations of the non-parametric damped Capon (dCapon) and APES (dAPES) spectral estimators introduced in [1]. The proposed estimators exploit efficient Gohberg-Semencul style formulations for the required matrix products and inverses, in combination with FFT-based fast trigonometric polynomial implementations of the nominator and denominator polynomials of the estimators. Numerical simulations illustrates the notable complexity gain of the proposed implementations.

$$\xi_{\omega,\lambda}(\mathbf{y}_M, \mathbf{w}_L) = \sum_{\kappa=0}^{M-1} \mathbf{f}_M^*(\omega,\lambda)\mathbf{Z}_M^\kappa \mathbf{y}_M \left(\mathbf{Z}_L^\kappa \mathbf{w}_L\right)^* \mathbf{f}_L(\omega,\lambda^{-1}) = \sum_{\kappa=0}^{M-1} \mathbf{f}_M^*(\omega,0)\mathbf{Z}_M^\kappa \mathbf{y}_M(\lambda) \left(\mathbf{Z}_L^\kappa \mathbf{w}_L(\lambda^{-1})\right)^* \mathbf{f}_L(\omega,0) \quad (41)$$

6. REFERENCES

[1] P. Stoica and T. Sundin, "Nonparametric NMR Spectroscopy," *J. Magn. Reson.*, vol. 152, pp. 57–69, 2001.

[2] J. R. Jensen, R. Heusdens, and S. H. Jensen, "A perceptual subspace approach for modeling of speech and audio signals with damped sinusoids," *IEEE Trans. Speech Audio Process.*, vol. 12, no. 2, pp. 121–132, March 2004.

[3] L. Lovisolo, E. A. B. da Silva, M. A. M. Rodrigues, and P. S. R. Diniz, "Efficient coherent adaptive representations of monitored electric signals in power systems using damped sinusoids," *IEEE Trans. Signal Process.*, vol. 53, no. 10, pp. 3831–3846, Oct. 2005.

[4] P. Stoica and R. Moses, *Spectral Analysis of Signals*, Prentice Hall, Upper Saddle River, N.J., 2005.

[5] X. Bai and B. He, "Estimation of Number of Independent Brain Electric Sources From the Scalp EEGs," *IEEE Trans. Biomed. Eng.*, vol. 53, no. 10, pp. 1883–1892, Oct. 2006.

[6] E. Gudmundson, P. Stoica, J. Li, A. Jakobsson, M. D. Rowe, J. A. S. Smith, and J. Ling, "Spectral Estimation of Irregularly Sampled Exponentially Decaying Signals with Applications to RF Spectroscopy," *J. Magn. Reson.*, vol. 203, no. 1, pp. 167–176, March 2010.

[7] F. J. Frigo, J. A. Heinen, J. A. Hopkins, T. Niendorf, and B. J. Mock, "Using Peak-Enhanced 2D-Capon Analysis with Single Voxel Proton Magnetic Resonance Spectroscopy to Estimate T2* for Metabolites," in *Proc. of ISMRM*, 2004, vol. 12, p. 2437.

[8] T. Kronvall, J. Swärd, and A. Jakobsson, "Non-Parametric Data-Dependent Estimation Of Spectroscopic Echo-Train Signals," in *Proceedings of the 38th IEEE International Conference on Acoustics, Speech and Signal Processing (ICASSP)*, 2013.

[9] A. Jakobsson, S. L. Marple, Jr., and P. Stoica, "Two-Dimensional Capon Spectrum Analysis," *IEEE Trans. Signal Process.*, vol. 48, no. 9, pp. 2651–2661, September 2000.

[10] T. Ekman, A. Jakobsson, and P. Stoica, "On Efficient Implementation of the CAPON Algorithm," in *Proc. of European Signal Processing Conference (EUSIPCO)*, Tampere, Finland, 2000.

[11] E. G. Larsson and P. Stoica, "Fast Implementation of Two-Dimensional APES and Capon Spectral Estimators," *Multidimensional Systems and Signal Processing*, vol. 13, no. 1, pp. 35–54, Jan. 2002.

[12] G.-O. Glentis, "A Fast Algorithm for APES and Capon Spectral Estimation," *IEEE Trans. Signal Process.*, vol. 56, no. 9, pp. 4207–4220, Sept. 2008.

[13] P. Stoica, A. Jakobsson, and J. Li, "Matched-Filterbank Interpretation of Some Spectral Estimators," *Signal Processing*, vol. 66, no. 1, pp. 45–59, April 1998.

[14] H. Li, J. Li, and P. Stoica, "Performance Analysis of Forward-Backward Matched-Filterbank Spectral Estimators," *IEEE Trans. Signal Process.*, vol. 46, no. 7, pp. 1954–1966, July 1998.